Description of Unbound States and in Terms of Unbound States

R. G. Lovas, T. Vertse and A. T. Kruppa

Yukawa Institute, Kyoto, 11 December, 2012

The rationale of my talk

- Review talk
- Intuitive review of discrete unbound states & examples
- Unbound states: objects or means of description
- Common in all discrete states: S-matrix poles
- Little novelty, but new light on the relationship of approaches
- Applications rationed sparingly to avoid overlap with Japanese contributors

Plan of the talk

1. Extended quantum mechanics
   1.1. States belonging to the S-matix poles
   1.2. The Berggren representation
   1.3. Variational method for resonances
   1.4. Scattering-state approximants
   1.5. Bound-state approximants
   1.6. Illustrative example for the Berggren representation
   1.7. Complex scaling
2. Applications
   2.1. Multicannel case, multiple poles
   2.2. Alpha decay
   2.3. Proton decay from deformed nuclei
   3.4. Isobaric analogue resonances in the Lane model

1. Extended quantum mechanics

1.1. States belonging to the S-matix poles

Analytic continuation of the physical problem to complex wave numbers and energies

Single particle in a real potential

$$\int dr\, u_1(r)\mathcal{O}u_2(r), \quad \text{if } u_1,\ \mathcal{O}u_2 \in L^2$$

Radial integrals unchanged if performed along paths rotated

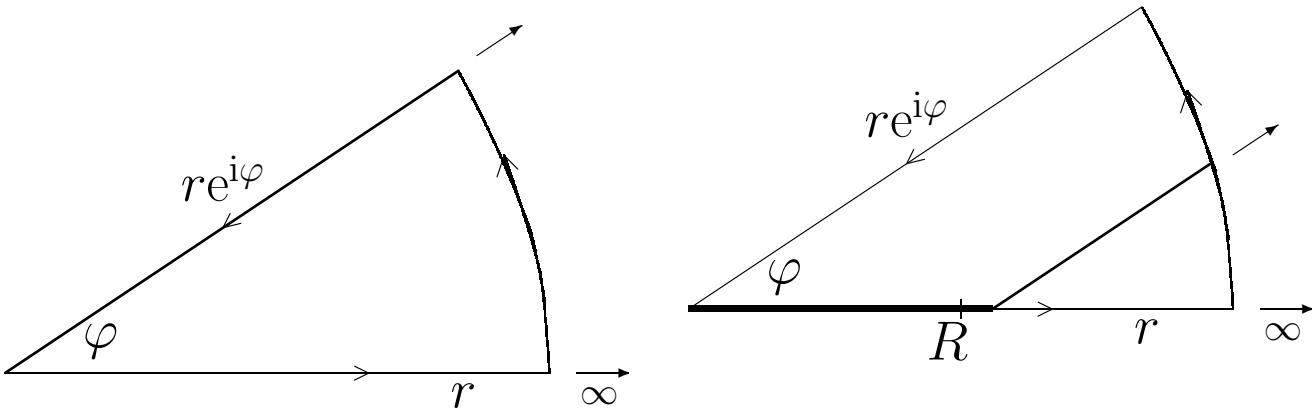

Alternative integration paths: thick lines

The asymptotic forms of $l = 0$ radial wave functions:

$$u(r) \sim \mathrm{e}^{-ikr} - S\mathrm{e}^{ikr} \quad \text{borrowed from scattering states}$$

S-matrix: $S = S(k)$ or $S = S(E)$ is a 1×1 matrix.

Generalizations to the multichannel case are trivial.

In a pole of the S-matrix the scattering wave function can be written to look like

$$u(r) \sim \mathrm{e}^{ikr},$$

where	$k = i\gamma$	for bound states,
	$k = \kappa - i\gamma$	for resonance (decaying) states,
	$k = -\kappa - i\gamma$	for antiresonance (capturing resonance) states,
	$k = -i\gamma$	for virtual (antibound) states $\quad (\kappa, \gamma \geq 0)$.

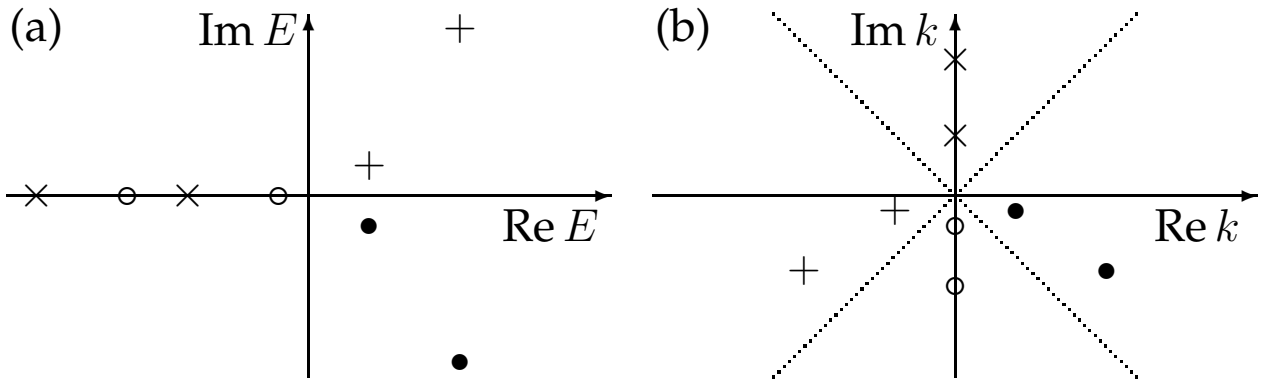

Poles of the S-matrix on the complex energy or momentum plane

bound states: $\times$;

virtual (antibound) states: $\circ$;

resonances or decaying states: $\bullet$;

antiresonances or capturing resonances: $+$.

resonances and antiresonances are each others mirror images

The poles migrate and change their natures when the parameters are varied:

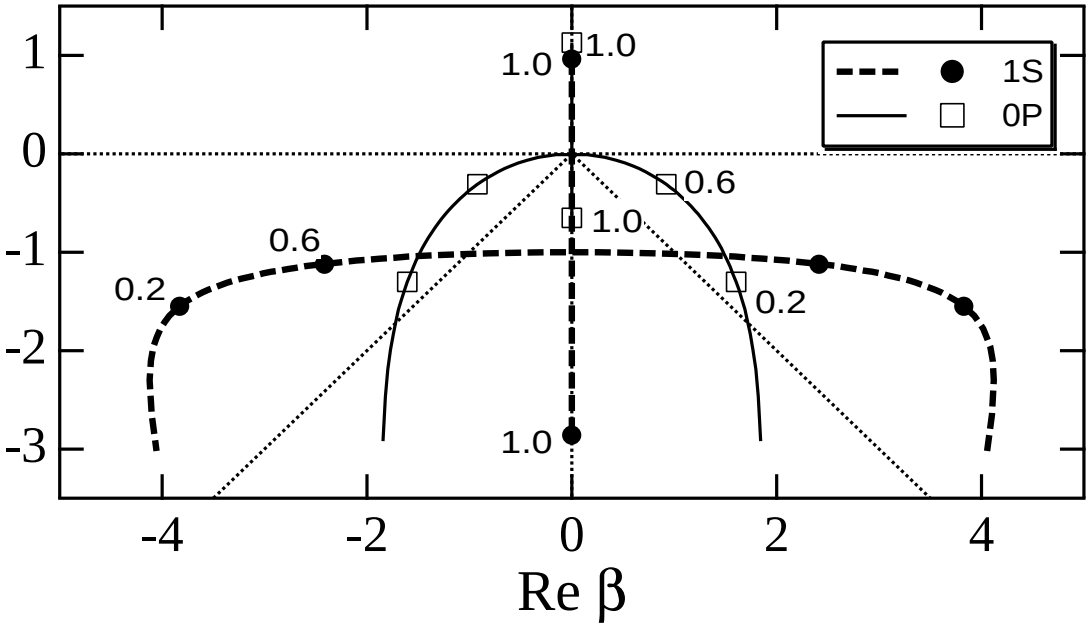

Some s- and p-wave S-matrix poles in a square-well potential of radius a in the complex $\beta = ka$ plane. The oblique lines mark $\mathrm{Im}\,\beta = \pm\,\mathrm{Re}\,\beta$. Some scaling factor values are displayed.

The asymptotic forms of wave functions analytically continued in k:

$$\begin{aligned} u(r) \sim \mathrm{e}^{ikr} &= \mathrm{e}^{-\gamma r} \text{ for bound states,} \\ &= \mathrm{e}^{\gamma r}\mathrm{e}^{i\kappa r} \text{ for resonance (decaying) states,} \\ &= \mathrm{e}^{\gamma r}\mathrm{e}^{-i\kappa r} \text{ for antiresonance (...) states,} \\ &= \mathrm{e}^{\gamma r} \text{ for virtual (antibound) states} \quad (\kappa, \gamma \geq 0). \end{aligned}$$

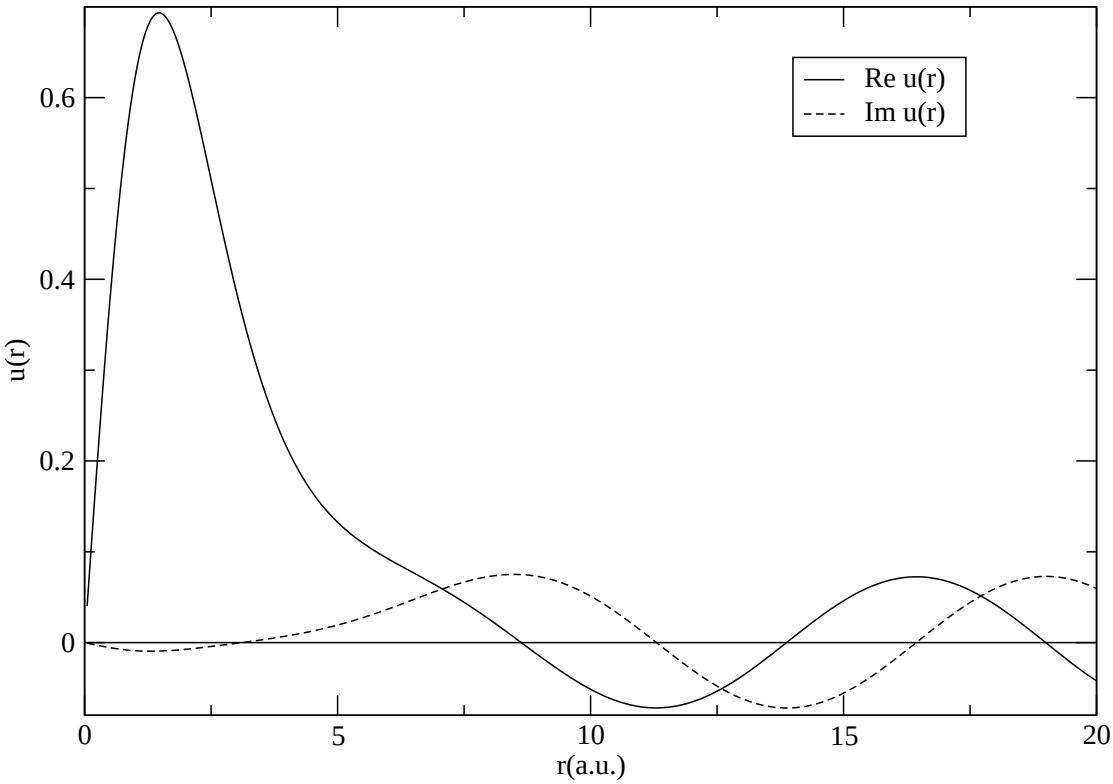

A typical resonance wave function (Gamow wave function). The amplitudes of oscillation increase exponentially. The antiresonance wave function differs only in the relative phase of the real and imaginary parts.

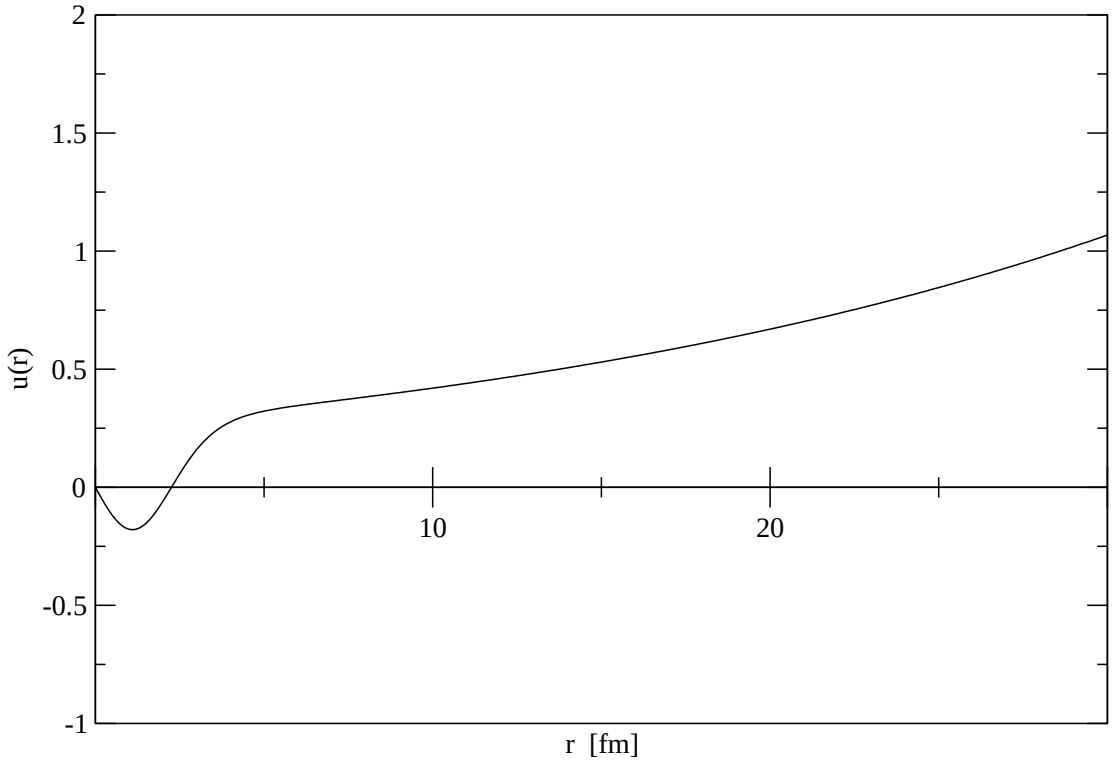

A typical virtual- (antibound-)state wave function. Its tail increases exponentially.

Since the unbound-state wave functions all diverge in infinity, their norms, overlaps and some of their matrix elements do not exist. However, if the unbound states are continued back into bound states, their matrix elements do exist, then the integration paths are distorted suitably, into complex, and the matrix elemets are unchanged; then they can be continued in k analytically, and the integrals do in general exist.

Symbolically:

$$u_{\mathrm{unbound}}(r) \Rightarrow u_{\mathrm{bound}}(r) \Rightarrow u_{\mathrm{bound}}(r\mathrm{e}^{i\varphi}) \Rightarrow u_{\mathrm{unbound}}(r\mathrm{e}^{i\varphi})$$

With the binding decreased, a bound state $u(r)$ is continued as a pair of resonance and antiresonance states $u(r)$, $\tilde{u}(r)$. The norm integral:

$$\langle u|u\rangle = \int dr\, u^*(r)u(r) \Rightarrow \int dr\, \tilde{u}^*(r)u(r) = \int dr\, u^2(r).$$

The norm integral exists and is unique if $\varphi > |\arg(k)|$:

$$\exp\left(ikr\mathrm{e}^{i\varphi}\right) = \exp\left[i|k|\mathrm{e}^{i(\varphi-|\arg(k)|)}r\right] \underset{r\to\infty}{\longrightarrow} 0 \qquad (k = |k|\mathrm{e}^{-i|\arg(k)|}). \tag{1}$$

With $\varphi > \pi$, even antibound states become tractable in this way.

The unbound states are not legitimate quantum mechnical states.

Physical meaning of a decaying resonance state (Gamow state):

Consider a stationary solution to $i\hbar\frac{\partial}{\partial t}\Psi = H\Psi$ for energy $\mathcal{E} = E - i\frac{1}{2}\Gamma$:

$$\left.\begin{aligned} i\hbar\tfrac{\partial}{\partial t}\Psi &= H\Psi \\ \Psi &= \mathrm{e}^{-\frac{i}{\hbar}\mathcal{E}t}\psi = \mathrm{e}^{-\frac{\Gamma}{2\hbar}t}\mathrm{e}^{-\frac{i}{\hbar}Et}\psi \\ |\Psi|^2 &= \mathrm{e}^{-\frac{\Gamma}{\hbar}t}|\psi|^2 \end{aligned}\right\} \Rightarrow \left\{\begin{array}{l} H\psi = \mathcal{E}\psi, \\ \psi(\mathbf{r}) \propto u(r) \sim \mathrm{e}^{ikr}, \end{array}\right.$$

The Hamiltonian H is only Hermitean on the Hilbert space;

$|\Psi|^2 \propto \mathrm{e}^{-\frac{\Gamma}{\hbar}t}$ describes exponential decay. The spatial dependence $u \sim \mathrm{e}^{\gamma r}\mathrm{e}^{i\kappa r}$ expresses that the decay was started infinitely long ago.

For an antiresonance (the time-reversed of a deacaying state) $|\Psi|^2 \propto \mathrm{e}^{\frac{\Gamma}{\hbar}t}$ describes a capture that was started infinitely long time ago.

In a multichannel scheme the Gamow state is an ideal deacying state, which forgot in which channel it was born, like Bohr's compound resonance.

1.2. The Berggren representation

Extended quantum mechanics: construction of complete bases

Ordinary completeness relies on a contour integral on the complex k-plane, with the contour

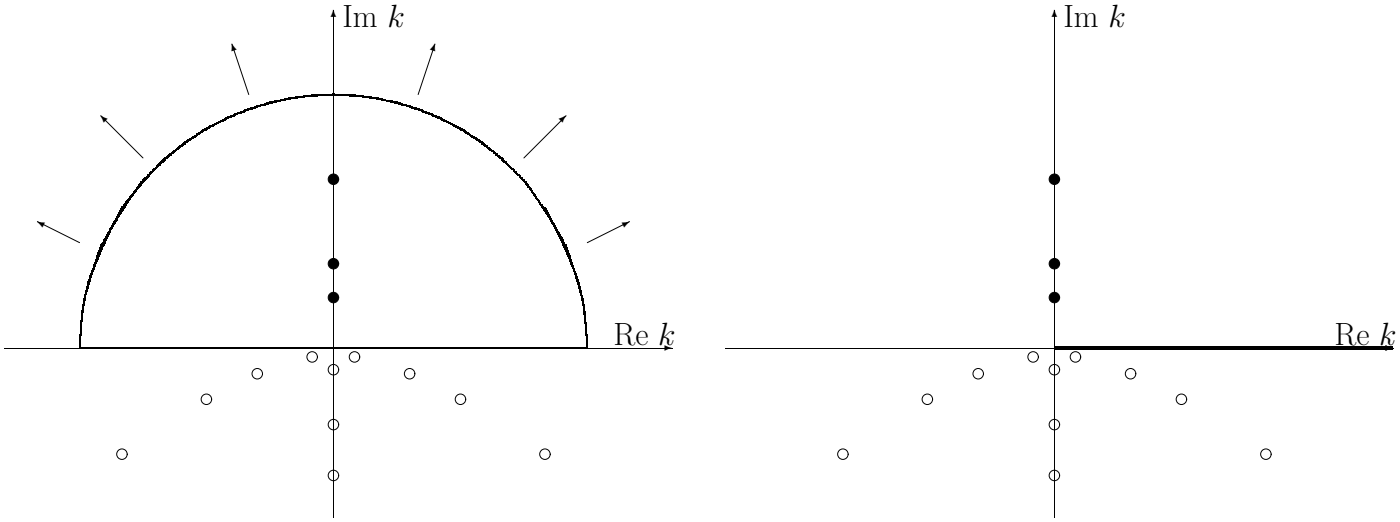

Contour for the proof of ordinary completeness (thick lines and full circles:

$$1 = \sum_n |u_n\rangle\langle u_n| + \frac{1}{\pi}\int_0^\infty dk |u_k\rangle\langle u_k|$$

The proof hinges on two things:

(i) the poles to be included are encircled,
(ii) the basis is (bi)orthonormal.

The contour thus may be distorted such that

(i) if the pole at k_n is encircled, that in $-k_n^*$ must be excluded;
(ii) if $|u_k\rangle$ is on the contour, then $|u_{-k}\rangle$ should also be there.

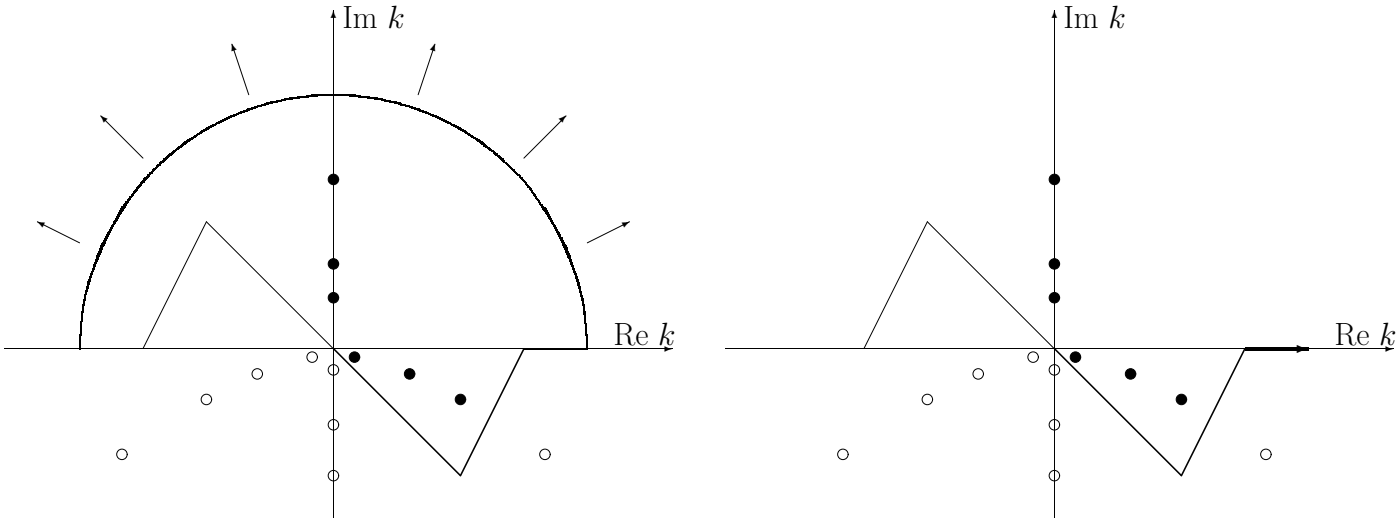

Beggren's contour and the Berggren basis (full circles and thick line)

With this, the completeness for a partial wave l looks like

$$\begin{aligned}\delta_l(r-r') &= \sum_n \tilde{u}_n^*(r)u_n(r') + \frac{1}{\pi}\int_0^\infty dk\, \tilde{u}_k^*(r)u_k(r') \\ &= \sum_n u_n(r)u_n(r') + \frac{1}{\pi}\int_0^\infty dk\, u_k(r)u_k(r').\end{aligned}$$

In fact, the trajectory need not return to the real k-axis, and may involve virtual states as well:

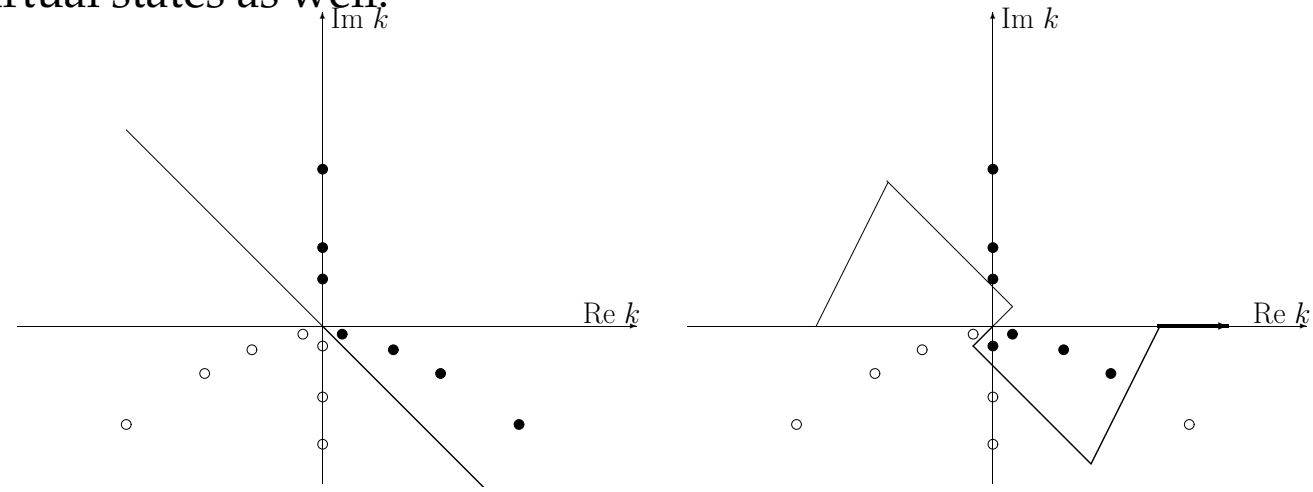

Berggren basis reminiscent of the figure of complex scaling and Berggren basis with a virtual state

The Berggren representation is based on a biorthogonal basis: the matrix elements always contain 'tilde'-d functions is bra position.

In fact, $\langle\tilde{u}|u\rangle$ an overlap of the resonance state with its time-reversed pair. What contributes to the overlap is the inner part of the wave function, and the oscillatory tail is projected out:

$$\langle\tilde{u}|u\rangle\!\!=\!\!\int_0^R dr\, u^2(r) + \int_R^\infty dr\, \mathrm{e}^{2ikr} = \int_0^R dr\, u^2(r) + 0 - \frac{\mathrm{e}^{2ikR}}{2ik}.$$

The resonance state normalized as in the Berggren theory is the resonance before decay.

The idea of a resonance is inherently vague $\Rightarrow$ complex physical quantities.

Im $\mathcal{E} \sim \Gamma$; Im $\mathcal{O} \sim$: inherent uncertainty

The Berggren representation: description of both unbound and bound states on equal footing

It can ce used in multichannel and multiparticle problems as well.

1.3. Variational method for resonances

Potential problem, trial function:

$$\psi = \sum_n c_n \phi_n(\boldsymbol{r}) + M\mathcal{O}_k(\boldsymbol{r}),$$

$$\phi_n(\boldsymbol{r}) \in L^2, \quad \begin{cases} \mathcal{O}_k(\boldsymbol{r}) \xrightarrow[r\to 0]{} 0 \\ \mathcal{O}_k(\boldsymbol{r}) \xrightarrow[r\to\infty]{} e^{ikr} \end{cases}, \quad k = \sqrt{(2m/\hbar^2)\mathcal{E}}$$

c_n and M variational parameters

Ritz-type trial function, but $\mathcal{O}$ depends on the energy to be determined. $\delta H = 0 \Rightarrow$

$$\begin{aligned} \sum_n c_n \langle \phi_m | H - \mathcal{E} | \phi_n \rangle + \langle \phi_m | H - \mathcal{E} | \mathcal{O}_k \rangle M &= 0 \\ \sum_n c_n \langle \tilde{\mathcal{O}}_k | H - \mathcal{E} | \phi_n \rangle + \langle \tilde{\mathcal{O}}_k | H - \mathcal{E} | \mathcal{O}_k \rangle M &= 0, \end{aligned}$$

Non-trivial solution:

$$\det \begin{Bmatrix} \langle \phi_m | H - \mathcal{E} | \phi_n \rangle, \langle \phi_m | H - \mathcal{E} | \mathcal{O}_k \rangle \\ \langle \tilde{\mathcal{O}}_k | H - \mathcal{E} | \phi_n \rangle, \langle \tilde{\mathcal{O}}_k | H - \mathcal{E} | \mathcal{O}_k \rangle \end{Bmatrix} = 0.$$

Transcendental equation for $\mathcal{E}$

Energy and wave function converges to the exact ones

Re $\mathcal{E}$ decreasing monotonously

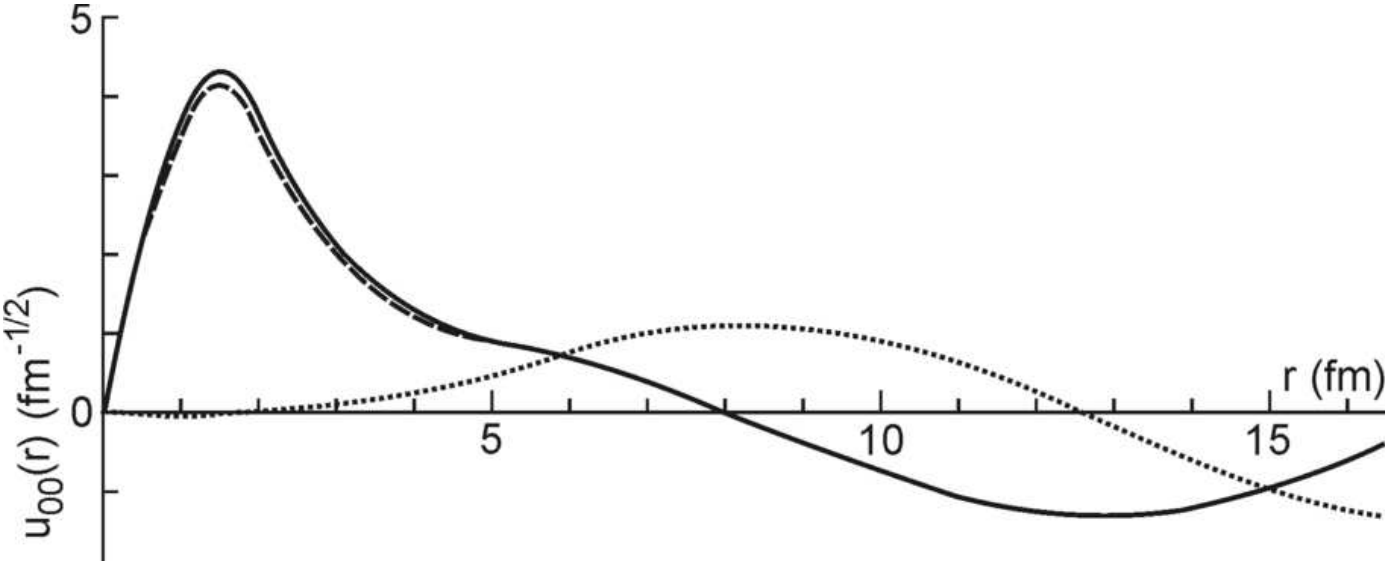

An approximate variational Gamow wave functions (with a poor basis) compared with the exact one

1.4. Scattering-state approximants

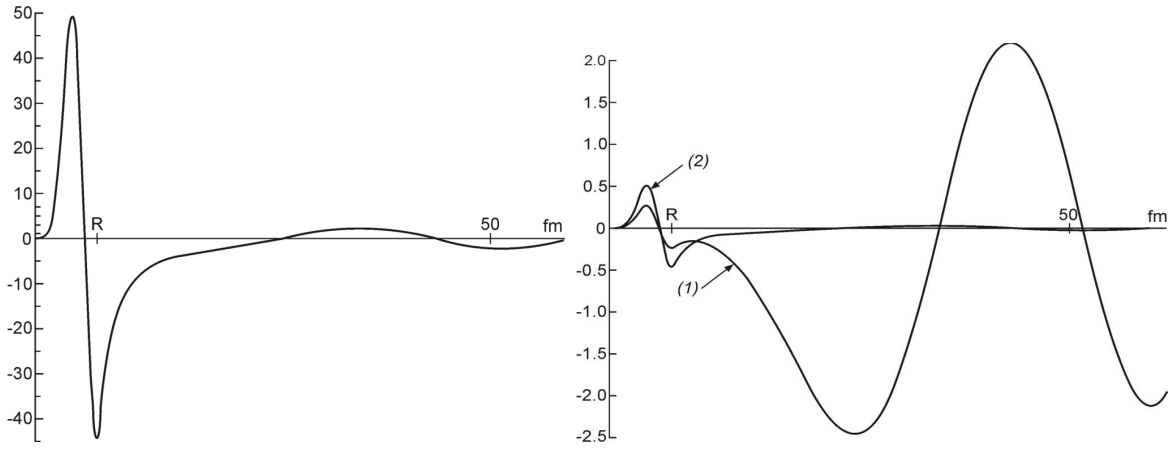

Real and imaginary parts of the Gamow wave function of a narrow resonance at $\mathcal{E}$, and of the scattering wave function at $\mathrm{Re}\,\mathcal{E}$. Note the different scales!

1.5. Bound-state approximants

Most common

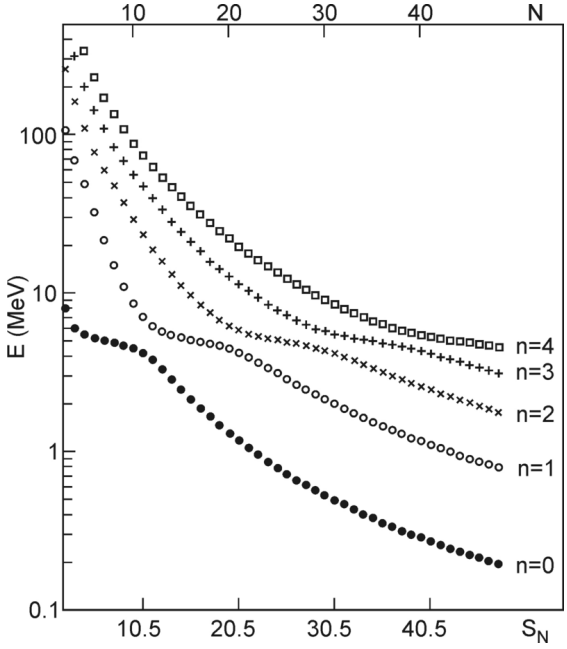

The lowest-lying energies on L^2 bases that span definite ranges S_N corresponding to different basis dimensions N

Exact energy: at the the inflexion points

All curves converge to 0 (i.e., the lowest-lying threshold)

The L^2 approximation to the wave funcion is best for bases belonging to the inflexion points:

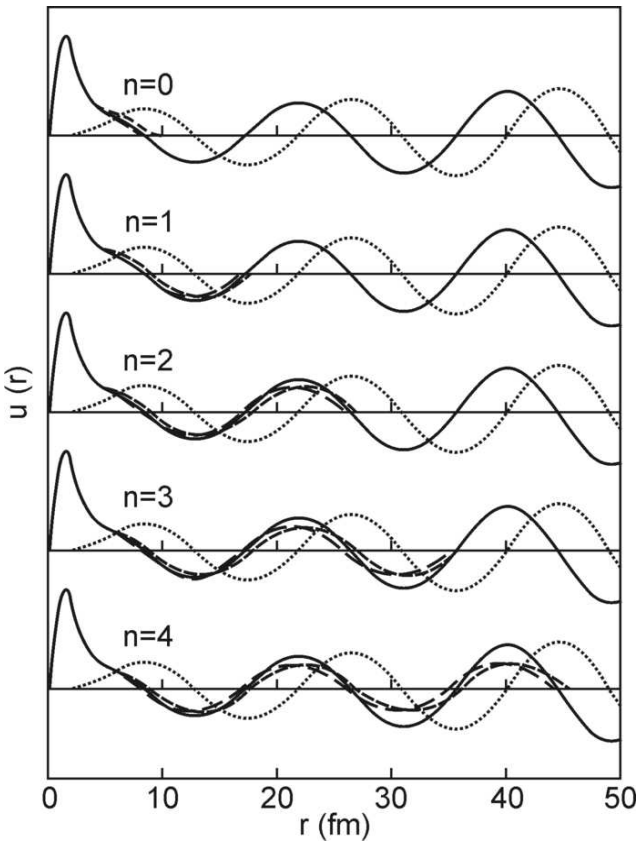

Gamow state versus bound-state-like approximants

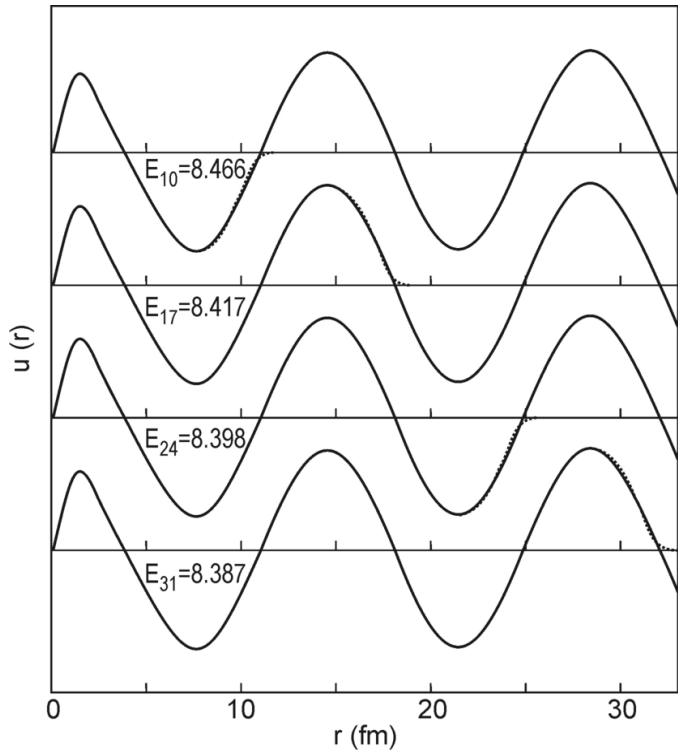

Resonance wave functions on L^2 bases compared with the scattering states at the same energies. The bases define box walls.

1.6. Illustrative example for the Berggren representation

The physical problem to be solved is

$$H = T + V, \quad V = \left[1 + \exp\left((r - r_0 A^{1/3})/a\right)\right]^{-1},$$
$$V_0 = -40.4 \text{ MeV}, \quad a = 0.6 \text{ fm}, \quad r_0 = 1.27 \text{ fm}$$

Basis: the eigenfunctions of the Hamiltonian

$$H_0 = T + U, \quad U = \left[1 + \exp\left((r - r_0 A^{1/3})/a\right)\right]^{-1},$$
$$U_0 = -44.4 \text{ MeV}, \quad a = 0.7 \text{ fm}, \quad r_0 = 1.27 \text{ fm}$$

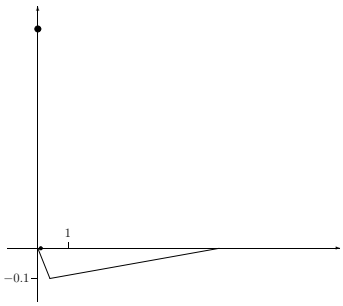

Basis for $h_{11/2}$: contour discretized (n equividistant ponts in each section) plus the two pole states

Convergence of the discrete states as functions of basis dimension $3n$

n	Bound state (MeV)	Resonance (MeV)
	-14.960	$2.251–0.026i$
0	$-12.517+0.001i$	$4.405–0.133i$
2	$-12.527+0.000i$	$4.081–0.275i$
4	$-12.527+0.000i$	$4.237–0.283i$
8	$-12.525+0.000i$	$4.305–0.314i$
16	$-12.526+0.000i$	$4.319–0.320i$
32	$-12.526+0.000i$	$4.321–0.321i$
128	$-12.526+0.000i$	$4.321–0.321i$
exact	–12.526	$4.321–0.321i$

The discretized values of the complex continuum converge to the contour at the same time.

The basis may be chosen not to embrace resonance poles. The resonance will then be produced by a superposition of complex continuum states.

1.7. Complex scaling

An alternative to the Berggren representation

$\boldsymbol{r}$ is rotated into the complex plane $\boldsymbol{r} \to \mathrm{e}^{i\theta}\boldsymbol{r}$ with $0 < \theta < \frac{\pi}{2}$, which transforms some resonance wave functions into square-integrable functions, while leaving the pole positions intact.

$U(\theta)$ acts like

$$\begin{aligned} U(\theta)\psi(\mathbf{r}) &= \exp\left[\tfrac{3}{2}i\theta\right]\psi[\mathbf{r}\exp(i\theta)], \\ H(\mathbf{r},\theta) &= U(\theta)H(\mathbf{r})U^{-1}(\theta) \end{aligned}$$

The tail of the Gamow wave function may transform into an exponentially damped (oscillatory) tail:

$$\exp\left(ik\mathrm{e}^{i\theta}r\right) = \exp\left[i|k|\mathrm{e}^{i(\theta-|\arg(k)|)}r\right] \quad (k = |k|\mathrm{e}^{-i|\arg(k)|}).$$

This is damped provided $\theta > |\arg(k)|$. Then the function is square-integrable.

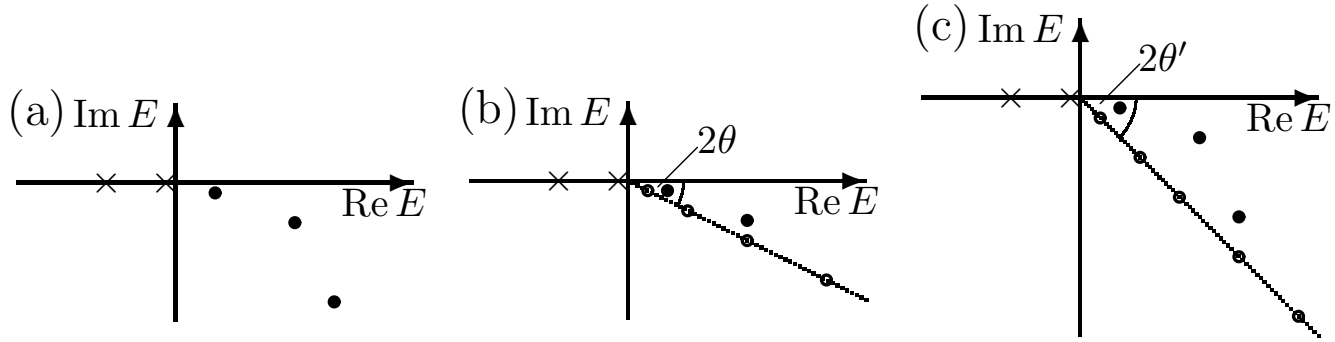

Bound-state ($\times$) and resonance ($\bullet$) poles in the complex energy plane without rotation (a), with rotation by θ (b), and by θ' (c). The discretized continuum eigenvalues are denoted by $\circ$. The energy continua are rotated by -2θ.

The energy continua are rotated by -2θ.

To see this, look at the asymptotic form resulting from the transformation: $r' = r\mathrm{e}^{i\theta}$;

introduce a new wave number, $k'_j = k_j \mathrm{e}^{i\theta}$:

$$u_j(r') \sim \delta_{ij}\mathrm{e}^{-ik_j r'} - S'_{ij}(k_j)\mathrm{e}^{ik_j r'} \sim \delta_{ij}\mathrm{e}^{-ik'_j r} - S'_{ij}[k_j(k'_j)]\mathrm{e}^{ik'_j r},$$

S': the transformed S-matrix

$k'_j = k_j \mathrm{e}^{i\theta}$ implies $E'_j = E_j \mathrm{e}^{2i\theta}$

E_j are the energies with respect to the nearest threshold from below

The asymptotic form of the rotated u' at k'_j is thus similar to that of the original problem at k_j.

Thus the continua are formed by the positive real values of E'_j.

$E_j = E'_j \mathrm{e}^{-2i\theta}$. It is thus plausible that the continua get rotated by -2θ.

The transformed problem is to be solved on an L^2 basis.

Some eigenenergies will belong to bound states and to resonances with $|\arg E_i| < 2\theta$

The rest will be discretized points of the rotated continua.

Resonances are distinguished by being stable against varying θ.

Complex scaling can be applied to complicated problems, but there are difficulties with broad resonances. There are also difficulties in back-rotating the wave function.

The matrix elements of $H(\mathbf{r}, \theta)$ are equal to those of $H(\mathbf{r})$ between basis states rotated by $-\theta$, which corresponds to -2θ in energy. That corresponds to the rotated continuum.

The same rotated continuum may be used in Berggren's representation as well:

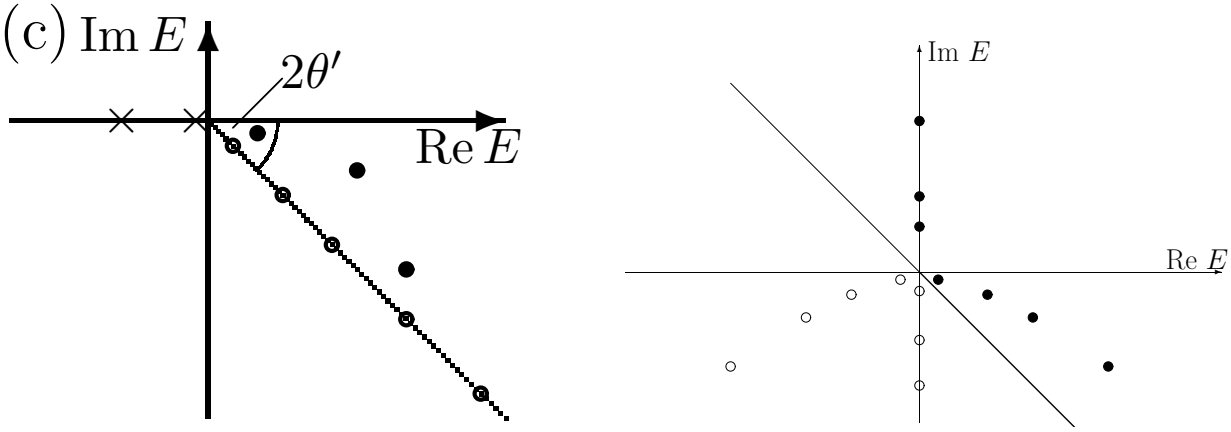

Comparison between a complex scaled and a similar Gamow basis

Differences:

- the actual forms of the basis along the rotated line are different;
- in the Gamow basis, Gamow states of a model problem are also to be included.

2. Applications

2.1. Multichannel case, multiple poles

$$u_1(r) \sim k_1^{-1/2}(\mathrm{e}^{-ik_1 r} - S_{11}\mathrm{e}^{ik_1 r}); \qquad k_1 \sim E^{1/2},$$
$$u_2(r) \sim -k_2^{-1/2} S_{12}\mathrm{e}^{ik_2 r}; \qquad k_2 \sim (E - \Delta E)^{1/2}.$$

The functions $S_{ij}[\mathcal{E}(k_1, \ldots, k_n)]$ are 2^n-valued functions because of the double values of each $k_i \sim \pm\sqrt{E_i}$.

The Riemann sheets for $\{S_{ij}[\mathcal{E}(k_1, \ldots, k_n)]\}$ as a function of the complex energy $\mathcal{E}(k_1, \ldots, k_n)$ may be characterized by

$$\{\text{sign}(\text{Im } k_1), \ldots, \text{sign}(\text{Im } k_n)\}.$$

The bound states are on the 'physical sheet' $\{+, \ldots, +\}$. The resonance poles are on the 'nearest' non-physical sheet, which is

$$\{-, \ldots, -, +, \ldots, +\},$$

where $-$ is associated with open, and $+$ with closed channels at energy $\text{Re}\,\mathcal{E}$.

(Sequence of channels: in growing order of the thresholds)

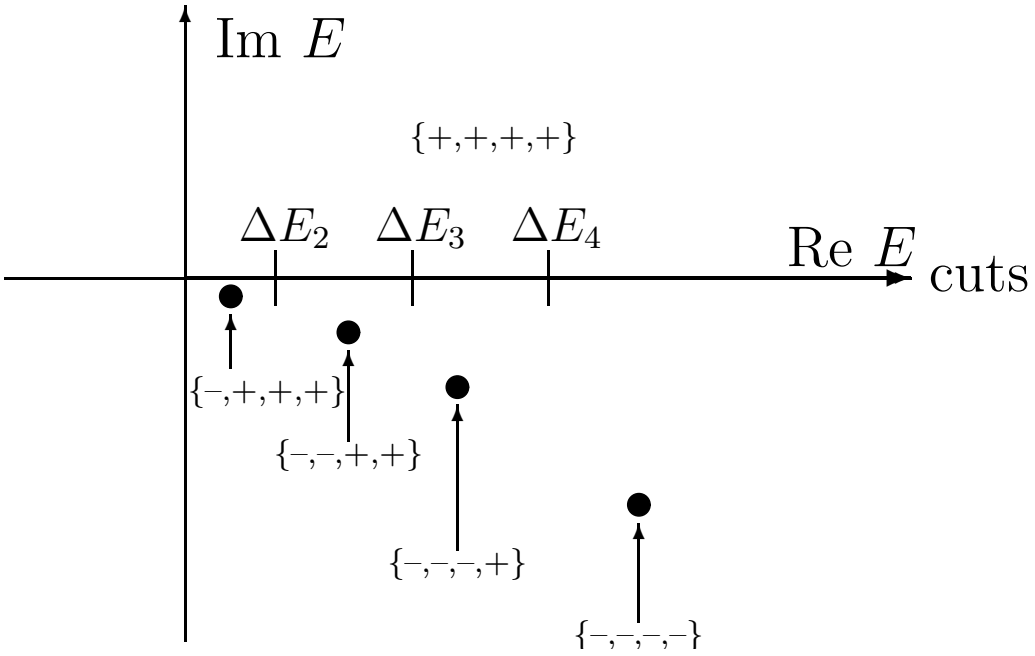

Thresholds ΔE_i, resonance poles and their Riemann sheets

n channels: 2^{n-1} poles belonging to each resonance.

Assume that in a one-channel system with a resonance at energy E_1 and wave number k_1. If another channel is coupled, the resonance pole will be on $\{-,-\}$, and there appear poles at (k_1, k_2) and $(k_1, -k_2)$

$\Longrightarrow$

- The resonance originates from channel 1 if the two pole locations are obtained from each other by $k_2 \to -k_2$.
- The resonance originates from channel 2 if the two pole locations are obtained from each other by $k_1 \to -k_1$.

The remote poles are called shadow poles. They duly disregarded in general.

In the $\frac{3}{2}^+$ resonance of ^{5}He, a shadow pole was found to contribute indicating that the resonance originates from the α+n channel, which is nonsense ($E_{\alpha+\mathrm{n}} = 17.7$ MeV, $E_{\mathrm{t+d}} = 60$ keV).

But the sign rule only applies to nearly zero coupling, and the strong coupling here causes the pole to migrate to another Riemann sheet.

The facts can be summed up as follows:

Riemann sheets (channel 1: α+n; channel 2: t+d):

- $(++)$ physical sheet
- $(--)$ sheet of the resonance pole for a resonance over the t+d threshold
- $(-+)$ sheet for a shadow pole belonging to a resonance originating from the first (α+n) channel; agrees surprisingly with the empirical finding
- $(+-)$ sheet for a shadow pole belonging to a resonance originating from the second (t+d) channel

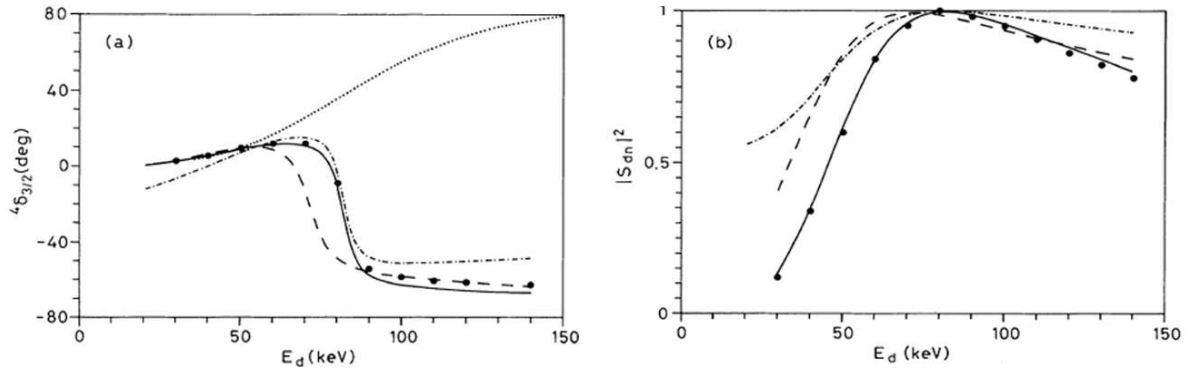

$^4S_{3/2}$ t+d phase shift and $|S_{dn}|^2$ in a pure t+d model (dotted) and in {α+n,t+d} models of different parameters

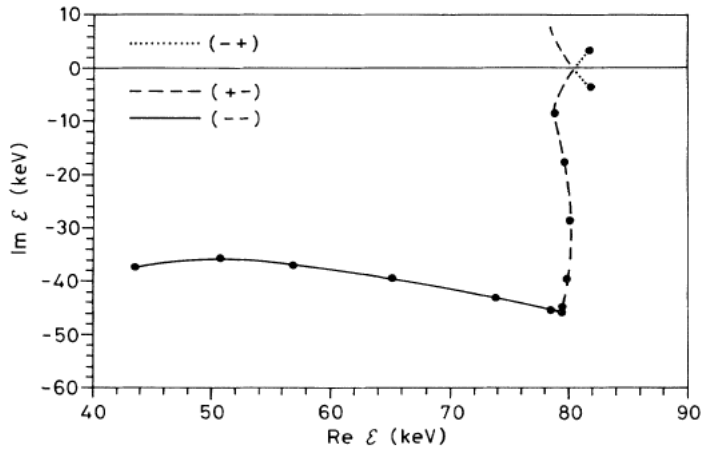

Trajectories of the two poles when the coupling is varied. The shadow pole walks from sheet $(+-)$ to sheet $(-+)$.

2.2. Alpha-decay

Many-particle problem, in which the projection of the wave function onto the decay channel $g_l(r)$ obeys an outgoing boundary condition.

The neck of the function decreases exponentially under the Coulomb barrier, and its complex tail starts oscillating beyond.

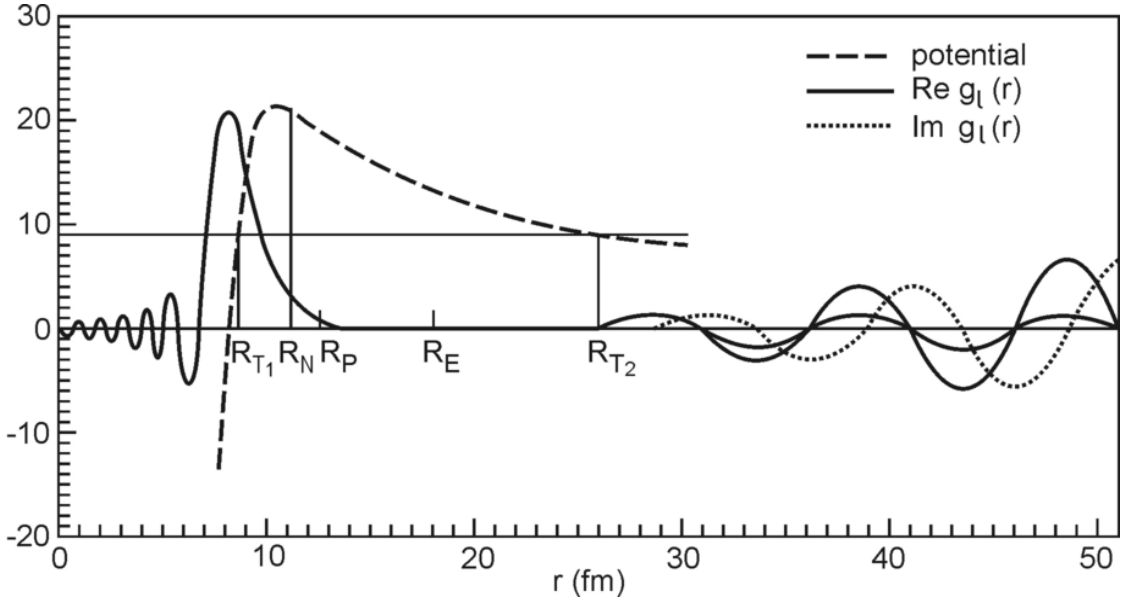

Projection of the wave function schematically; the size and rate of increase of the Gamow tail grossly exagerrated

The energy $\mathcal{E} = E - \frac{i}{2}\Gamma$ obtained by solving the complex eigenvalue problem carries information on the width (life-time).

Since $\mathrm{Im}\,\mathcal{E}/\mathrm{Re}\,\mathcal{E}$ may range from 10^{-10} to 10^{-30}, it requires enormous accuracy.

The same information in the neck of the Gamow function,

and that can be very well approximated in an L^2 basis.

That can be used in the R-matrix formula for the width

$$\Gamma = 2P_l(r_\mathrm{c})(\hbar^2/2\mu)g_l^2(r_\mathrm{c}),$$

g_l is the projection of the wave function on the decay channel,

P_l is the penetrability,

r_c should be in a region where there is only Coulomb interaction, but the nuclear structure calculation is still accurate enough.

^{212}Po $\longrightarrow$ ^{208}Po+α has been described satisfactorily in a shell + cluster model.

The absolute decay width has been reproduced: $\Gamma = 1.5 \times 10^{-15}$ MeV (Exp.: $\Gamma = 1.52 \times 10^{-15}$ MeV).

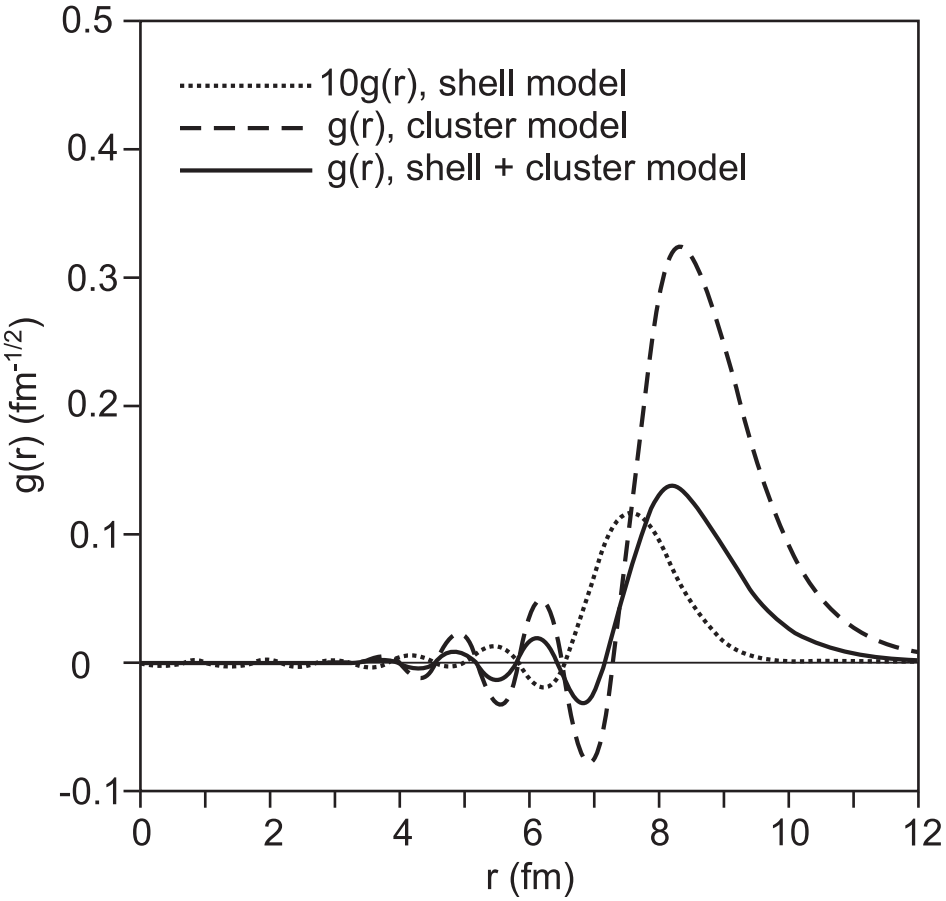

^{212}Po $\longrightarrow$ ^{208}Po+α. Projection on the decay channel in three models

2.3. Proton decay from deformed nuclei

Sevaral coupled open channels

Coupled-channels scheme based on a collective rotational model of the daughter.

Similar to the collective model for proton elastic and inelastic scattering, but outgoing boundary condition in all channels

The total wave function Ψ^{JM} expanded in terms of daughter states Φ_{J_d}

Coefficients $u^J_{J_d l_p j_p}$: the proton-daughter relative motion:

$$\Psi^{JM} = \frac{1}{r} \sum_{J_d j_p j_p} u^J_{J_d l_p j_p}(r) [\mathcal{Y}_{l_p j_p} \Phi_{J_d}]_{JM}.$$

$$\left[-\frac{\hbar^2}{2\mu} \frac{d^2}{dr^2} + \frac{\hbar^2 l_p(l_p+1)}{2\mu r^2} + V_\alpha(r) - E_\alpha \right] u^J_\alpha(r) + \sum_{\alpha'} V^J_{\alpha,\alpha'}(r) u^J_{\alpha'}(r) = 0$$

$$(\alpha = \{J_d j_p j_p\}).$$

Ground-state band of ^{141}Ho and ^{131}Eu;
extremely narrow states (τ: milliseconds, $\Gamma \sim 10^{-20}E$)

Various versions of collective models (rotational with Coriolis coupling, rot + γ vibrations)

The outgoing boundary contition was explicitly imposed, and Γ extracted

With complications mounting, an R-matrix approach was used for the calculation of Γ

The results are improving, but no conclusive result as yet

2.4. Isobaric analogue resonances (IAR) in the Lane model

Example for the complex shell model as well as for the complex scaling.

The Lane model: two-state ansatz for the target (or core) plus proton

$$\Psi = \Phi_{T_0 T_0}\phi_p|\tfrac{1}{2}-\tfrac{1}{2}\rangle + \Phi_{T_0 T_0-1}\phi_n|\tfrac{1}{2}\tfrac{1}{2}\rangle$$

and Hamiltonian

$$H = H(\xi) + \left[-\frac{\hbar^2}{2\mu}\frac{d^2}{dr^2} + \frac{l(l+1)}{r^2}\right] + V_0(r) + V_1(r)\boldsymbol{T}\cdot\boldsymbol{t} + V_C(r)(\tfrac{1}{2} - t_3),$$

$H(\xi)$: core Hamiltonian;

$T_0 T_0,\ T_0 T_0 - 1,\ \tfrac{1}{2}\tfrac{1}{2},\ \tfrac{1}{2}-\tfrac{1}{2}$: isospins & projections

Lane equations:

$$\left\{\left[-\frac{\hbar^2}{2\mu}\frac{d^2}{dr^2}+\frac{l(l+1)}{r^2}\right]+V_0(r)-\frac{T_0}{2}V_1+V_C-\mathcal{E}_p\right\}\phi_p+\sqrt{\frac{T_0}{2}}V_1\phi_n=0,$$

$$\left\{\left[-\frac{\hbar^2}{2\mu}\frac{d^2}{dr^2}+\frac{l(l+1)}{r^2}\right]+V_0(r)+\frac{T_0-1}{2}V_1-(\mathcal{E}_p-\Delta_C)\right\}\phi_n+\sqrt{\frac{T_0}{2}}V_1\phi_p=0.$$

Δ_C: Coulomb energy shift

With the coupling omitted,

$$\left\{\left[-\frac{\hbar^2}{2\mu}\frac{d^2}{dr^2}+\frac{l(l+1)}{r^2}\right]+V_0(r)-\frac{V_1}{2}T_0+V_C-\mathcal{E}_p^{(m)}\right\}\phi_p^{(m)}=0,$$

$$\left\{\left[-\frac{\hbar^2}{2\mu}\frac{d^2}{dr^2}+\frac{l(l+1)}{r^2}\right]+V_0(r)+\frac{T_0-1}{2}V_1-\mathcal{E}_n^{(m)}\right\}\phi_n^{(m)}=0.$$

The functions ϕ_p and ϕ_n can be expanded in terms of Berggren bases,

$$\phi_p^{(m)}=\sum_m C_p^{(m)}w_p^{(m)},\qquad \phi_n^{(m)}=\sum_m C_p^{(n)}w_n^{(n)}.$$

where $w_p^{(m)}$ and $w_n^{(n)}$ belong to poles or to one of the discretized elements of the continuum.

The Lane equations can be solved on the basis $\{w_p^{(m)}, w_n^{(m')}\}$:

$$(\mathcal{E}_p^{(m)} - \mathcal{E}_p)C_p^{(m)} + \sqrt{\frac{T_0}{2}} \sum_{m'} \langle \tilde{w}_p^{(m)} | V_1 | w_n^{(m')} \rangle C_{m'}^{(n)} \; = \; 0,$$

$$(\mathcal{E}_n^{(m)} - \mathcal{E}_n)C_n^{(m)} + \sqrt{\frac{T_0}{2}} \sum_{m'} \langle \tilde{w}_n^{(m)} | V_1 | w_p^{(m')} \rangle C_{m'}^{(p)} \; = \; 0.$$

Alternatively, the one-body 2×2 matrix Hamiltonian implicit in the Lane equations can be rotated into the complex plane, and the two results can be compared with the resonance parameters extracted by a direct numerical solution of the Lane equations. To this end, the screened Coulomb potential should be chosen to have the 'dilation-analytic' form:

$$V_C(r) = Ze^2 \frac{\mathrm{Erf}(r/\alpha)}{r}, \text{ with } \alpha = 0.31 \text{ fm}.$$

IAR energies and widths for ^{209}Bi in MeV with the Berggren basis, complex scaling (CS) and with the solution of the Lane equations

lj	E_r			Γ		
	Berggren	CS	Lane	Berggren	CS	Lane
$g_{9/2}$	14.933	14.933	14.934	0.041	0.041	0.042
$i_{11/2}$	15.493	15.493	15.493	0.002	0.002	0.002
$d_{5/2}$	16.436	16.436	16.444	0.121	0.120	0.120
$s_{1/2}$	16.913	16.913	16.913	0.127	0.127	0.128
$g_{7/2}$	17.350	17.349	17.349	0.076	0.075	0.074
$d_{3/2}$	17.434	17.434	17.433	0.118	0.119	0.120
$j_{15/2}$	18.752	18.751	18.752	0.005	0.005	0.005

Berggren bases (open circles for neutrons and squares for protons) and the results (filled circles) for the $g_{9/2}$ resonance in ^{209}Bi

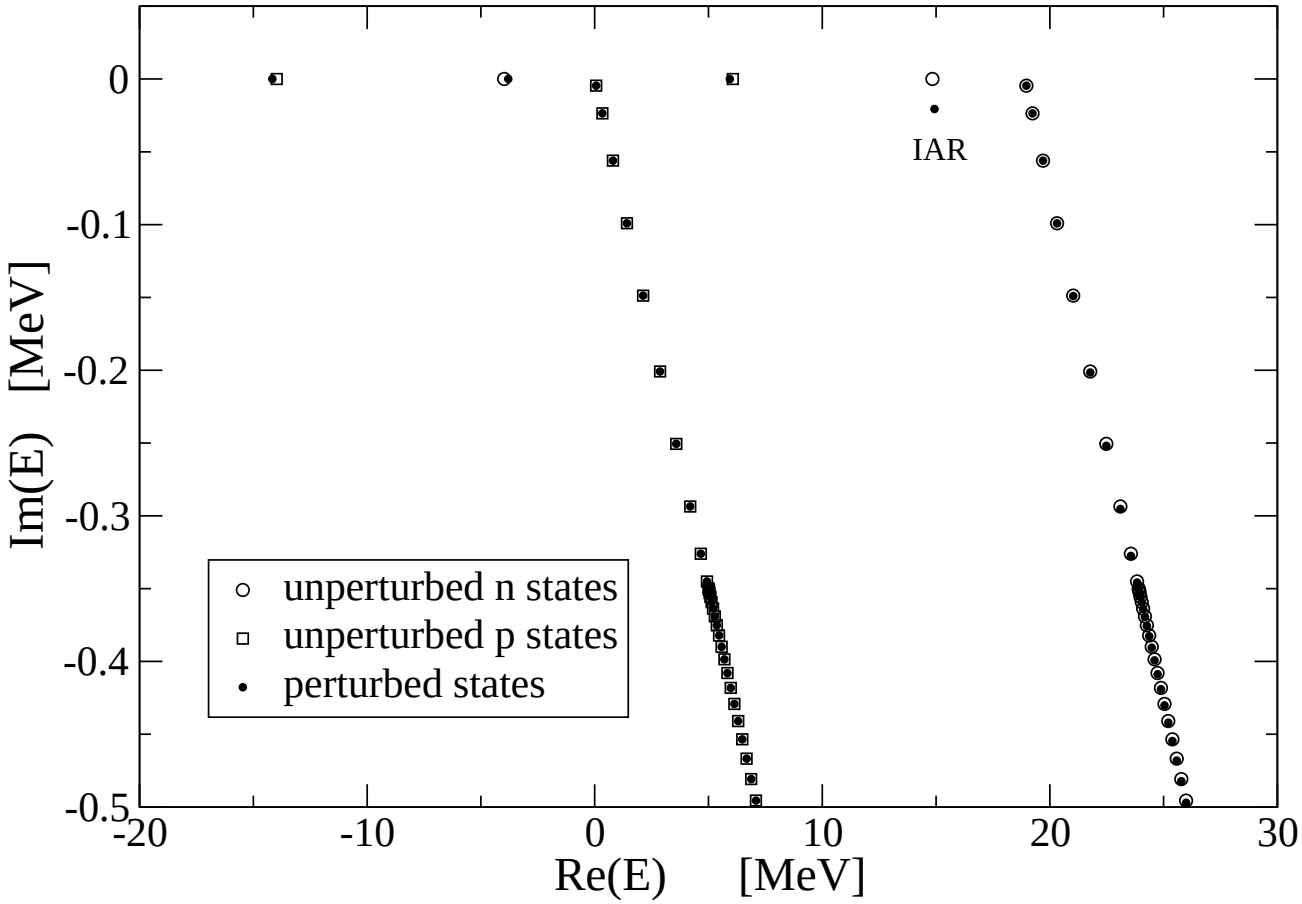

These trajectories are the same as used for complex scaling. The two methods give the same results for all physical states within 1 keV.

This conclusion appropriately crowns this review.